Single-shot surface profiling by multi-wavelength interferometry without carrier fringe introduction

Katsuichi Kitagawa*

Toray Engineering Co. Ltd., 1-1-45, Oe, Otsu, 520-2141, Japan

ABSTRACT

As a single-shot interferometric technique, spatial carrier interferometry has been thoroughly investigated, and it has been shown to have some problems, such as low spatial resolution. To overcome the problems, we propose a novel single-shot surface profiling technique that does not require carrier introduction. It is based on a model-fitting algorithm and estimates the model parameters and the heights of plural points simultaneously based on their multi-wavelength intensity data. The validity of the proposed method is demonstrated by computer simulations and actual experiments.

Keywords: Interferometry, single-shot, carrier fringe, surface profile, multi-wavelength

* E-mail: katsuichi_kitagawa@toray-eng.co.jp

This is an extended version of a paper titled "Multiwavelength single-shot interferometry without carrier fringe introduction" presented at QCAV2011 in Saint-Etienne, France.

1. Introduction

The measurement accuracy of interferometric surface profiling is generally limited by environmental vibration. This is because the conventional methods use multiple images with different reference positions. To overcome this problem, researchers developed single-shot interferometry, which can measure the surface profile from a single image. A typical example is spatial carrier interferometry, in which carrier fringes are introduced by tilting the reference mirror. From a single interferogram, the phase distribution can be calculated by the Fourier-transform method [1], the spatial synchronous method [2-3] or the Local Model Fitting method [4]. However, spatial carrier interferometry has the disadvantages of low spatial resolution and a limited measurable slope angle. Also, this technique requires a long coherence length illumination source and optics with long depth-of-focus imaging.

Another approach is the so-called fringe pattern analysis method, which detects the modulating phase from a single interferogram that contains possible closed fringes. A fringe pattern can be generally modeled as follows:

$$I(x,y) = A(x,y) + B(x,y)\cos\{\phi(x,y)\}, \tag{1}$$

where $I(x, y)$ is the observed intensity, $A(x,y)$ is the background intensity, $B(x,y)$ is the fringe amplitude and $\phi(x, y)$ is the desired phase distribution. If the background intensity can be removed and the fringe amplitude can be normalized, the fringe pattern can be written as

$$I(x,y) = \cos\{\phi(x,y)\}. \tag{2}$$

In this case, the phase is obtained by

$$\phi_0(x,y) = \arccos\{I(x,y)\}, \tag{3}$$

where $\phi_0(x, y) \in [0,\pi]$ is the principle value of the arccosine function [5-6]. However, this technique is limited in its application because of the following requirements: The fringe density must be high enough to get a correct

normalized pattern, and the surface must be smooth enough that the sign of the arccosine function can be determined by assuming the smoothness and continuity of the estimated phase. Furthermore, it is impossible to determine whether the surface is concave or convex for a closed fringe pattern.

To resolve the drawbacks just described, we propose a new algorithm for single-shot interferometry that does not require spatial carrier fringe introduction. This technique is called the Global Model Fitting (GMF) method, and its most significant feature is that there is no loss in spatial resolution. We proved the validity of the GMF method by computer simulations and actual experiments.

2. Principle of the GMF method

Our algorithm consists of two steps; a flowchart is shown in Fig. 1. Step 1 is the GMF method, which estimates the surface height of each pixel from its color information. Because of the high computational cost, this method is applied to a limited number of pixels in practical use. Step 2 is another method, named ACOS, which calculates the heights of the other pixels in a shorter time, by using the information obtained from Step 1. The information can also be applicable to other images captured under the same optical conditions. For that reason it can be called a recipe.

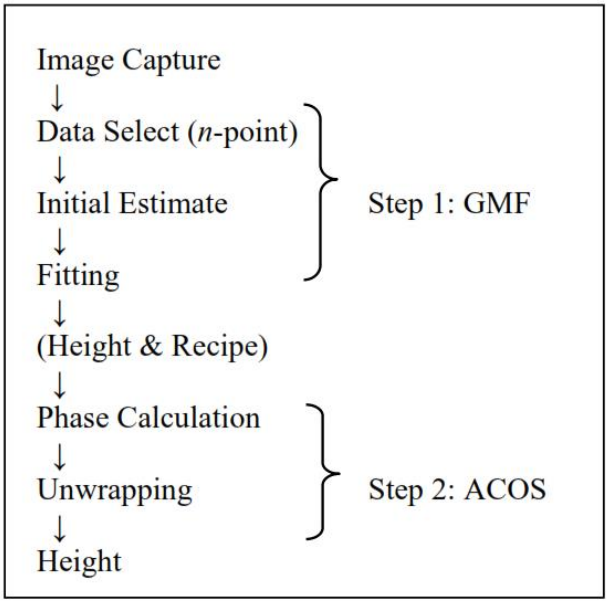

Figure 1. Flowchart of the proposed method.

2.1 The GMF method

2.1.1 Relation between color and height in three-wavelength interferometry

Let's consider an optical configuration for the three-wavelength single-shot interferometry shown in Fig. 2. This is almost the same configuration as that reported by Kitagawa [7]. With this optics we can capture an interferometric color image as shown in the upper part of Fig. 3. This image was experimentally obtained with a slightly tilted surface as shown in the lower graph, where the straight line represents the height and the curves represent the BGR intensities. Please note that the color change is due to the cyclic variation of BGR signals according to the optical path difference (OPD) between the test and reference surfaces. This means that we can estimate the surface height of each pixel from its color information. This interference color phenomenon is the same as that seen in soap bubbles. Its typical application is transparent film thickness measurement, where the white-light interference color is analyzed by spectroscopy.

The principle drawback of white-light systems is that they are just too slow. The solution to this problem is

to settle on a small number of discrete wavelengths and measure the corresponding intensities directly, rather than scanning through the spectrum. One example already proposed is the head slider flying height measurement system described by Kubo et al.[8], in which a color camera captures the interference image and the flying height at each pixel is estimated from its hue. The relation between hue and the flying height must be obtained in advance.

Similarly it would be possible to estimate the surface profile from the color image based on calibration data obtained in advance using a test surface with known heights [9]. However, there would be two problems with such a scheme. One is determining how to estimate the height from the color, and the other is that the relationship between height and color can change easily depending on the optics and surface conditions. To overcome these problems, we propose a new technique, described in the next section.

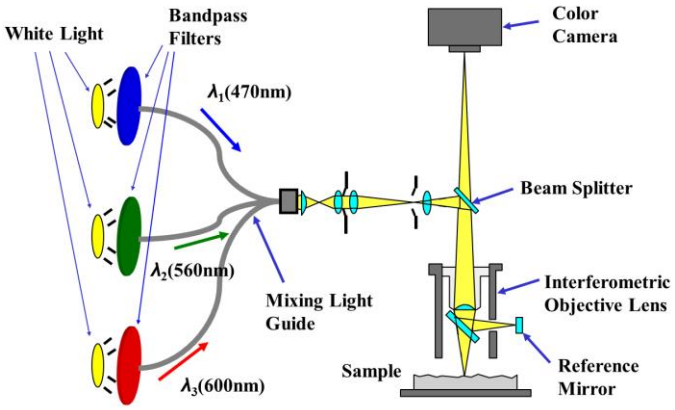

Figure 2. Optics of three-wavelength single-shot interferometry.

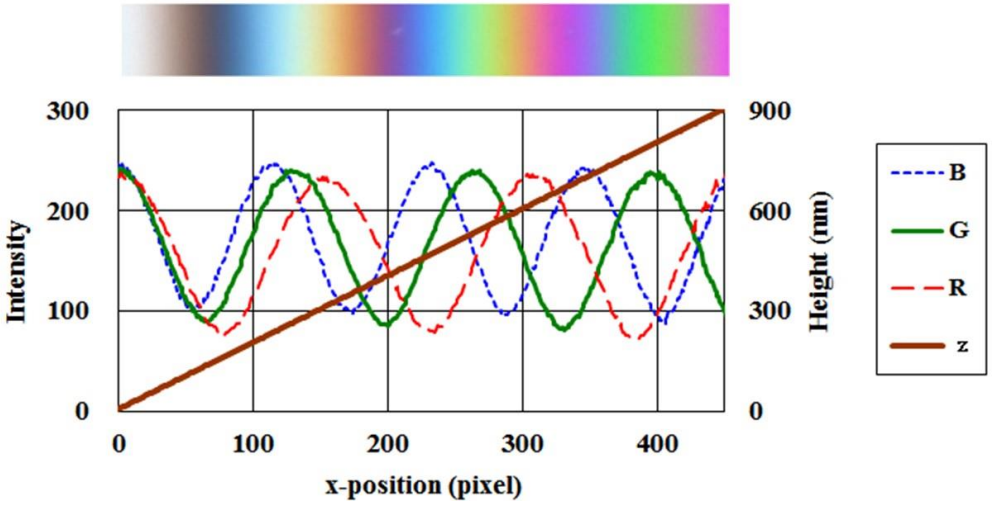

Figure 3. Relation between color and surface height in three-wavelength interferometry.

2.1.2 The GMF algorithm

There are three wavelengths in Fig. 2 and Fig. 3, but in the following equations we assume a more generalized expression of m wavelengths. The interferometric intensity is given by the following model:

$$g(i, j) = a(j)[1 + b(j)\cos\{\phi(i, j)\}], \tag{4}$$

where $g(i, j)$ is the intensity at point i ($i = 1, 2, \ldots, n$) and wavelength j ($j = 1, 2, \ldots, m$), $a(j)$ and $b(j)$ are the average value and the modulation of the waveform, respectively, and $\phi(i, j)$ is the phase given by

$$\phi(i, j) = 4\pi z(i) / \lambda_j, \tag{5}$$

where $z(i)$ is the height relative to the zero OPD, and λ_j is the wavelength of the wavelength number j.

Equation (4) can be expressed by

$$g(i, j) = a(j)[1 + b(j)\cos\{4\pi z(i) / \lambda_j\}]. \tag{6}$$

This model is derived under the assumption that the waveform parameters $a(j)$ and $b(j)$ are constant in the field of view (FOV) and dependent only on the wavelength. This assumption will be almost always valid when the target surface is homogeneous.

The unknown parameters $a(j)$, $b(j)$ and $z(i)$ can be estimated using the following least-square fitting equation:

$$J[a(j), b(j), z(i)] = \sum_{i=1}^{n} \sum_{j=1}^{m} \left[g(i, j) - g_{ij} \right]^2, \tag{7}$$

where $g(i, j)$ is the model intensity defined by Eq. (6) and g_{ij} is the observed intensity.

This non-linear least-square problem can be solved by any numerical methods. In this paper, we used the Solver program in MS Excel for the computer simulation. For the actual experiments, we used our own program based on the Davidon-Fletcher-Powell algorithm.

2.1.3 Necessary conditions

Let us consider the necessary conditions to obtain the unknown parameters $a(j)$, $b(j)$ and $z(i)$. When the number of wavelengths is m and the number of points is n, the total number of unknown parameters is $2m+n$. Since m values are observed at one point, the necessary condition for the solution is $mn \geq 2m + n$. Then, the number of points must be

$$n \geq 2m/(m-1) \tag{8}$$

This means $n \geq 4$ in the case of $m = 2$, and $n \geq 3$ in the case of $m = 3$. When $n = 2m/(m-1)$, then the problem becomes a $(2m+n)$-order non-linear simultaneous equation, and when $n > 2m/(m-1)$, then the problem becomes a $(2m+n)$-order non-linear least-square problem.

Figure 4 illustrates the principle of this algorithm in the case of three wavelengths and n-points. From $3n$ observed intensities, $(n+6)$ unknown parameters, i.e., n-point heights and six waveform parameters, are estimated.

Please note that the least-square fitting problem becomes ill-conditioned if the intensity values of the selected points are limited to a narrow range. However we can easily avoid this situation by tilting the target surface even when it is completely flat.

There is one important detail we must take care of. As shown in Fig. 3, the color is symmetrical along the zero OPD. Therefore, it is essential to make the OPD only positive or negative everywhere in the FOV by adjusting the *z*-axis.

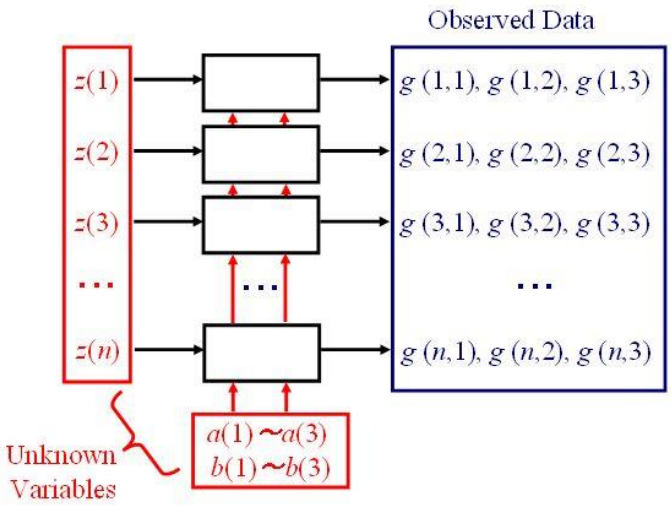

Figure 4. Principle of the GMF method (in the case of 3 wavelengths and *n*-point fitting)

2.1.4 Initial estimates

To find solutions to the non-linear least-square problem described in the previous section, we use an iterative gradient-based optimization technique, which requires initial estimates that will allow us to search for the minimum. Since the model function of Eq. (6) contains a cosine function, the error function has a lot of local minima. Therefore, it is essential to make good initial estimates.

In this paper, $a(j)$ is set to be the average of the observed values and the modulation, $b(j)$, is set to be the range of observed values divided by $2a(j)$. The height, $z(i)$, is a rough estimate which is given usually by a priori knowledge of the target surface.

2.2 The ACOS method

The computational cost of the non-linear least-square problem is very high. For example, in our experiment

shown in Section 3, the required calculating time for 100-pt GMF fitting was approximately 60ms using a C language program running on a 3.4GHz Intel Core i7-2600 CPU. This means it would be more than 150s for 512 × 480 pixels. Therefore, we use the GMF algorithm as the first step with a small number of points, for example, under one hundred, and then the heights of the other points are calculated as the second step by the ACOS method described below.

2.2.1 Phase estimation

Since the waveform parameters are obtained from Step 1, the phase can be calculated from the observed intensity by the following equation derived from Eq. (4):

$$\phi(i, j) = \arccos[\{g_{ij} / a(j) - 1\} / b(j)], \tag{9}$$

where $\phi(i, j) \in [0,\pi]$ is the principle value of the arccosine function. When the argument of the function is not within [−1, 1], the function is undefined. In this case, the argument is approximated as −1 or 1.

2.2.2 Phase unwrapping

From the phase, the height, $z(i, j)$, is obtained by

$$z(i, j) = [\pm\phi(i, j) / 2\pi + N(i, j)](\lambda_j / 2), \tag{10}$$

where $N(i, j)$ is the fringe order (integer), which is estimated by the coincidence method [7]. The principle of this method is the same as the so-called exact fractions method [10] for gauge block length measurement by multi-wavelength interferometry.

Figure 5 shows an experimental example of using this method. For each wavelength, the heights with different orders are plotted. The unknown orders are determined so that the three candidate heights match best. In this case, the height is estimated as 510 nm. It should be noted that the phase is obtained by the arccosine function, not by the arctangent function. Therefore, there are two candidate heights for each fringe order, as shown in Fig. 5.

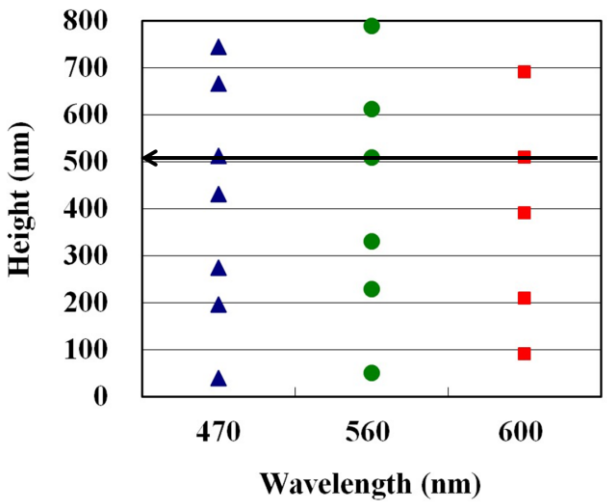

Figure 5. Phase unwrapping by the coincidence method.

3. Computer Simulations

3.1 Test method

A three-wavelength interferometric color image was synthesized with the following conditions: (a) image size = 50×50 pixels; (b) pixel size = 1 μm; (c) wavelength = 470, 560, 600 nm; (d) target surface = sphere with 1-mm radius, with a small square protrusion of height 50 nm and size 4×4 pixels; (e) waveform parameters of a = 100 and b = 1. The target surface is shown in Fig. 6(a), and the synthesized image is shown in Fig. 6(b). All the computations were done in MS Excel with a Windows PC. The non-linear least-square fitting in the GMF method was executed by the Solver program in MS Excel.

We performed two experiments. The first one used 3 points for fitting, and the second one used 50 points. The coordinates of the sampled points were (5, 25), (15, 25), (25, 25) in the first test and (1, 25), (2, 25), …, (50, 25) in the second test.

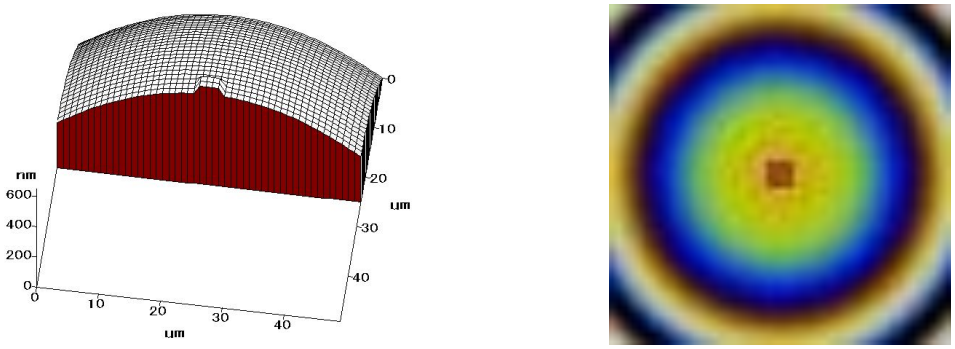

(a) Target surface (cross-sectioned) (b) Synthesized color image

Figure 6. Target surface and its color fringe image used for computer experiments.

3.2 Test results

3.2.1 Three-point fitting

The BGR images are shown in Fig. 7 with three points used for fitting. The intensity values are shown in Fig. 8(a). The initial estimates of the heights are set at 95% of the true ones. The data for fitting and the results are shown in Table 1 and Fig. 8(b), respectively. The parameters and heights are estimated correctly.

Next, we estimated the height profile of 50 points along the $y = 25$. The intensities and calculated phases are shown in Fig. 9(a)(b). The heights are estimated almost correctly, as shown in Fig. 10.

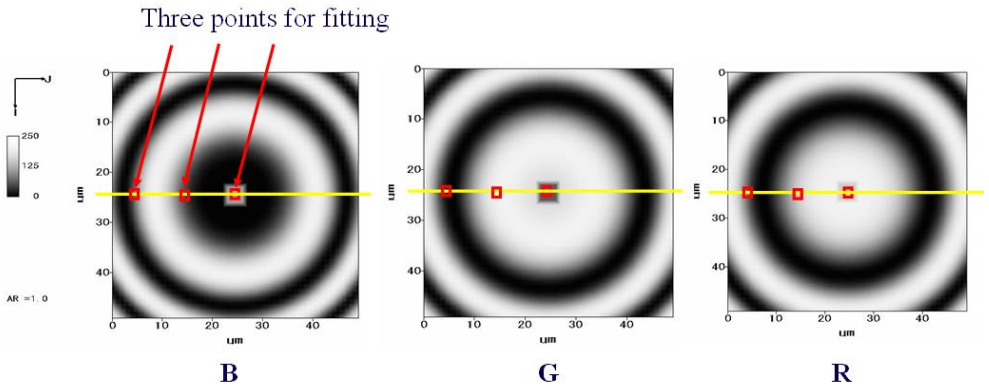

Figure 7. Fringe images of three colors and three points used for fitting.

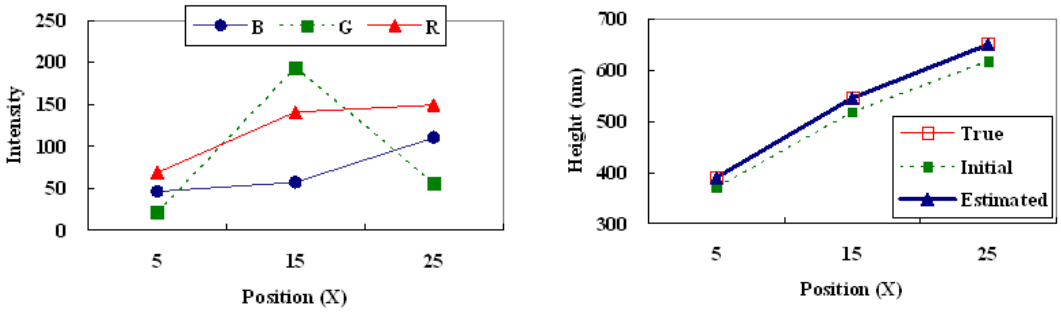

(a) Intensities of 3 points (b) Heights of 3 points

Figure 8. Observed intensities and the estimated height by the 3-point fitting.

Table 1. Estimated results by the 3-point fitting.

Parameters		True	Initial	Estimated	Error(%)
z	*z*(1)	390.2	370.7	390.1	-0.01
	z(2)	545.2	517.9	545.2	0.00
	z(3)	650.2	617.7	650.2	0.00
a	*B*	100	78.5	100.1	0.05
	G	100	108.1	100.0	-0.03
	R	100	109.2	100.0	-0.05
b	*B*	1.00	0.41	0.999	-0.06
	G	1.00	0.80	1.000	0.04
	R	1.00	0.37	1.001	0.06

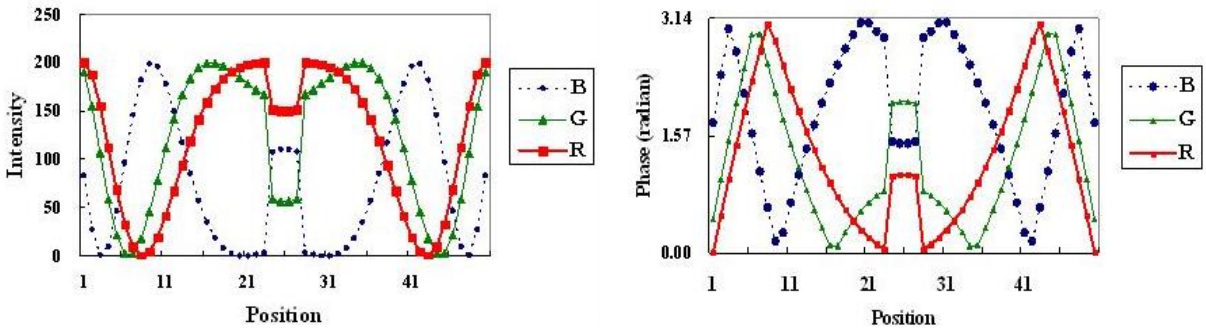

(a) Intensity profiles of 50 points along $y = 25$ (b) Phase profiles calculated by the ACOS method

Figure 9. Observed intensities and phase profiles in the second step.

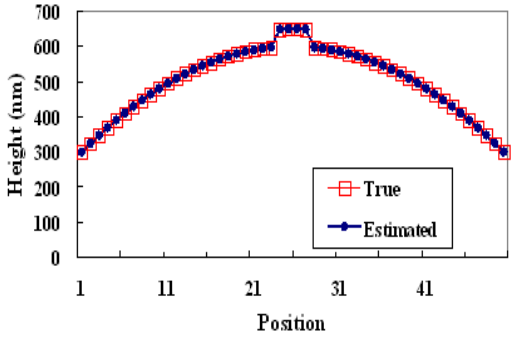

Figure 10. Estimated heights of 50 points by the ACOS method with the recipe obtained by the GMF 3-pt fitting.

3.2.2 50-point fitting

We estimated the height profile of 50 points along the $y = 25$ using 50 points for the GMF fitting. The intensities are shown in Fig. 9(a). The initial estimates are set to be the true heights minus 50 nm. The heights are estimated correctly, as shown in Fig. 11. Please note that the small protrusion of 4×4 pixel size is measured correctly without any loss in spatial resolution.

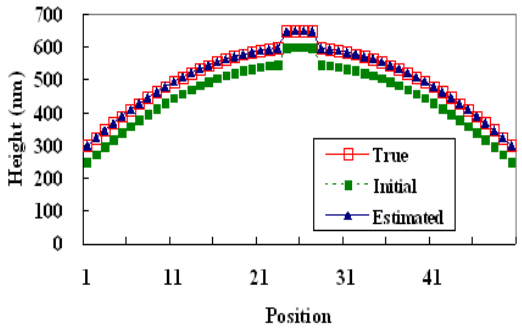

Figure 11. Estimated heights of 50 points by the GMF 50-pt fitting.

4. Actual Experiments

4.1 Test method

We installed the GMF algorithm in the optical surface profiler SP-500 by Toray Engineering Co., Ltd. (Fig.

12) [11], some of which was modified for three-wavelength single-shot interferometry as follows. The illumination unit was three halogen lamps, three narrow-band filters with 10-nm bandwidth and a mixing light guide with three branches, as shown in Fig. 2. The central wavelengths of the filters were 470 nm, 560 nm and 600 nm. The camera was a three-CCD color camera with 1360 × 1024 pixels. The captured image data was stored in a PC memory as an integer value from 0 to 255. The color crosstalk was compensated by the crosstalk compensation algorithm reported by Kitagawa [7].

We measured the surface profile of a 50-nm step height. The surface was slightly tilted so that the interference image had different colors in the field of view, as shown in Fig 13. For simplicity we calculated the central portion of 512 × 480 pixels of the captured image. The non-linear least-square equation in the GMF algorithm was solved using the Davidon-Fletcher-Powell method [12]. The data for fitting were 20 points of $x = 25, 50, 75, \ldots, 500$ and $y = 240$. In the second step, we calculated the height of the whole area of 512×480 pixels by using the parameters obtained in the first step.

Figure 12. Surface profiler used for experiments.

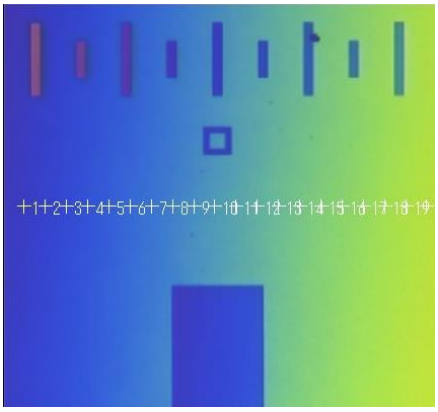

Figure 13. Captured color fringe image of 50-nm step height (512 × 480 pixels) and 20 sampled data points (shown in white numbers).

4.2 Test results

The 20-point intensity data are shown in Fig. 14. From these data, the heights of 20 points were estimated by the GMF method as shown in Fig. 15. The results agree with the expected flat surface. Then the heights of the whole area were measured by the ACOS method, and the results are shown in Fig. 16 and Fig. 17. Notice that the bottom areas of small slits are measured without smoothing out sharp edges. This shows the significant feature of the proposed technique that there is no loss in spatial resolution. It has been impossible by the conventional spatial carrier interferometry. Another advantage is its measurement speed. The total calculation time for 512 × 480 pixels was about 200ms including 4ms of the GMF fitting using a C language program running on a Windows PC with 3.4GHz Intel Core i7-2600 CPU. Because the calculation of the ACOS method is pixel-independent, the speed would be very much improved by a parallel processing technique.

The tests results have proved the validity of the proposed method. However, we can notice some errors in the results. To solve this problem and to extend the measurement range are still be investigated.

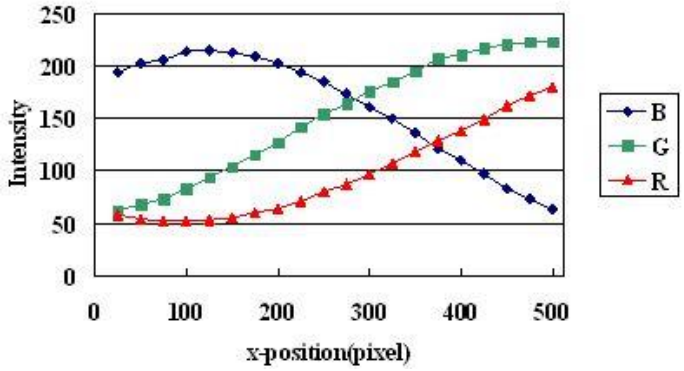

Figure 14. BGR intensity data of 20 points used for fitting.

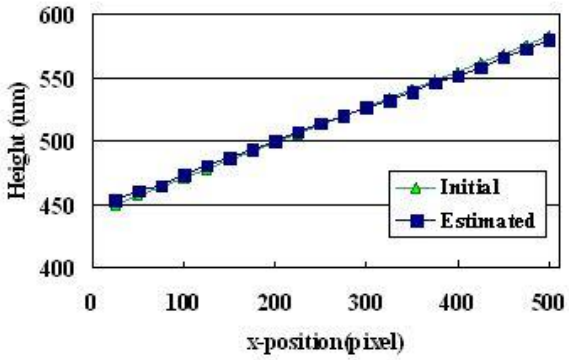

Figure 15. Estimated heights of 20 points obtained by the GMF method.

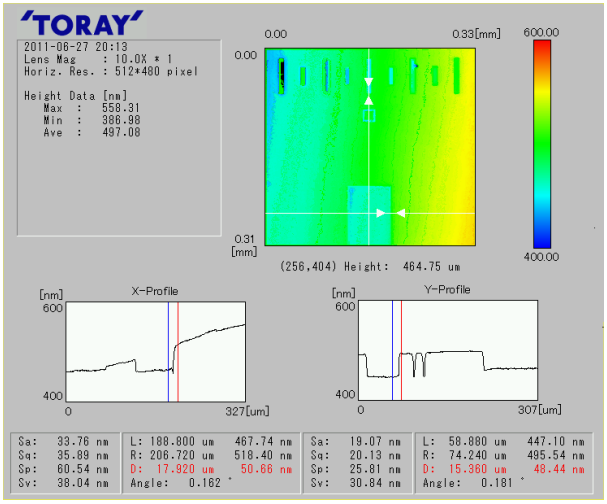

Figure 16. Estimated heights at 512 × 480 pixels by the ACOS method. The upper panel is a 3-dimensional map, and the lower graphs show *x*- and *y*-profiles.

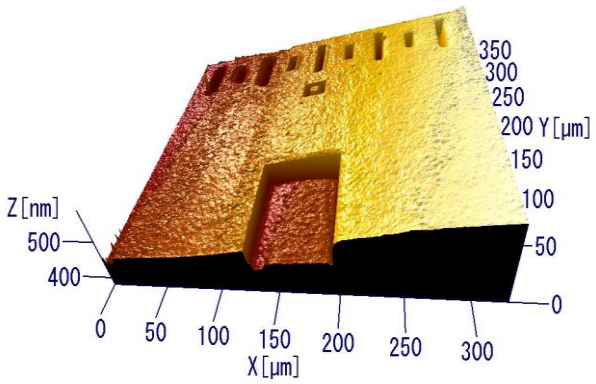

Figure 17. Estimated heights of the 50-nm step height in 3D view.

5. Discussion

5.1 Horizontal resolution

Both the GMF method and the ACOS method estimate the surface height of each pixel from its color information without using any information about its neighboring points. Therefore, there is no loss in spatial resolution. This feature has been proved by a computer simulation (Fig. 11) and an actual experiment (Fig. 16, Fig. 17).

5.2 Vertical resolution

What is the height measurement accuracy of the GMF method? This is an important, non-trivial question that leads to an analysis of the algorithm. Since the GMF method determines plural heights and waveform parameters simultaneously, it would be too complex to make a complete analysis. Therefore, we focus here on estimating the effect of the observed intensity error on the height estimation.

In the GMF method, the estimated height of each point is mostly dependent on the intensity of the point, because in this method the error function of Eq. (7) is the sum of squared errors (SSE) of n points, and each error is independent from the heights of other points. In other words, the height, $z(i)$, is determined so that the model intensity, $g(i,j)$, becomes equal to the observed intensity, g_{ij}. This situation is the same as what occurs in the ACOS method.

In the ACOS method, the height is obtained by Eq. (10). Substituting Eq. (9) into Eq. (10) and omitting the fringe order term and variables i and j for simplicity, we obtain

$$z(g) = \pm(\lambda / 4\pi)\arccos\{(g-a)/ab\}. \tag{11}$$

The dependence of the height on the intensity, that is, the sensitivity coefficient, is then expressed by the following partial derivative:

$$\begin{aligned} c &= \left|\partial z(g)/\partial g\right| \\ &= \left|(\lambda/4\pi)(1/ab)/\sqrt{1-\{(g-a)/ab\}^2}\right|. \end{aligned} \tag{12}$$

This equation causes a division by zero. We can avoid this situation in the following way. In practical situations, the intensity of each point is obtained as a digital integer value, for example, between 0 and 255 in the case of 8-bit data length. Therefore, the sensitivity coefficient can be approximated by

$$c = \left|z(g+1) - z(g)\right|. \tag{13}$$

Figure 18 shows the height and its sensitivity coefficient as a function of the intensity when a=100, b=1 and λ = 600 nm. Although c is dependent on the intensity, it is mostly less than 1 nm/digit and its average is 0.75 nm/digit. Therefore, in the proposed method, we can expect approximately 1-nm height resolution and accuracy to within a few nanometers, provided that the noise level of the observed intensity is within a few gray levels.

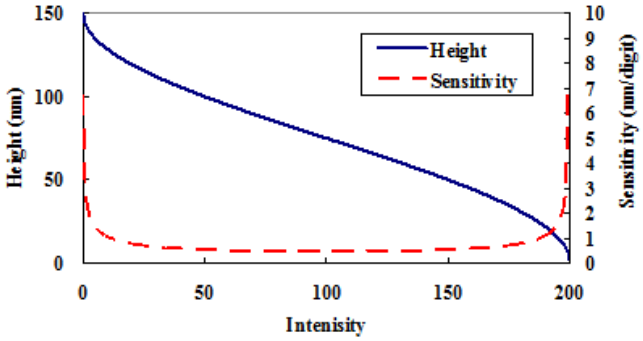

Figure 18. Plot of the height and its sensitivity coefficient as a function of the intensity.

5.3 Maximum acceptable height discontinuity

In the GMF method, the height of each pixel is determined directly without calculating its phase. This means that there is no phase unwrapping required and there is no sign ambiguity problem of the arccosine function. Therefore, theoretically there is no limit in the height discontinuity, provided that the height is within the measurable range, which is described in 5.4.

In the ACOS method, the height is determined by spectral unwrapping using the phases of three wavelengths, not by the spatial unwrapping. Therefore, the situation is the same as what occurs in the GMF method.

5.4 Maximum measurable height

In the GMF method, theoretically there is no limit to the height range. We note that the estimated height is dependent on its initial estimate, as discussed in 5.5.

The issue of the maximum measurable height of the ACOS method is almost the same as that with three-wavelength spatial carrier interferometry [7], because the height is determined by spectral unwrapping using the phases of three wavelengths. The range depends on various factors, including wavelengths, electronic noises and optical errors. As for the wavelengths, the 470-560-600 nm combination used in this

paper was selected by Kitagawa [7] as the optimum one for extending the height range to 4 μm. We measured the surface profile of a 50-nm step height in our actual experiment. To extend the measurement range is left for a future investigation.

5.5 Effect of the initial estimates

As mentioned in 2.1.4, the error function has a lot of local minima. Therefore, it is necessary to start with the best initial estimates possible for the parameters to avoid getting trapped in local minima. To do this, we must investigate the problem of how accurately the parameters must be estimated to get the true solution. For this purpose we first made a theoretical analysis and then validated its result by a numerical experiment.

Although there are many unknown parameters in the least-squares fitting of Eq. (7), only the height parameters, $z(i)$, are inside the cosine function and can cause multiple local minima in the error function. Furthermore, since the error function is the sum of squared errors of n points, its relation to the estimated height of one point is independent of the estimated heights of the other points. Therefore, we focus here on obtaining the relation between the error function and the height of one point, assuming that the heights of the other points and the waveform parameters are all correctly fixed. Hence the error function is expressed as follows:

$$SSE = \sum_{j=1}^{m} e_j^2, \tag{14}$$

where e_j is the intensity error defined as

$$e_j = g_j(z) - g_j(z_0), \tag{15}$$

where z_0 is the true height, and

$$g_j(z) = a_j[1 + b_j \cos(4\pi z / \lambda_j)]. \tag{16}$$

Figure 19 shows the intensity error of each wavelength as a function of the height, when a_j=100, b_j=1,

z_0=500nm and the wavelengths are 470, 560 and 600 nm. We obtain the relation between the error function *SSE* as a function of the height, as shown in Fig. 20. The relations for various true heights are obtained similarly. Figure 21 shows the *SSE* versus the height estimate error δz (= z - z_0) for the true heights of 200, 300,…, 800 nm. From this figure, it can be concluded that the initial estimate of the height must be within ±100 nm of the true value. Otherwise, the searched optimum solution will be one of the local minima, which is at least 200-300 nm apart from the true height.

To validate this analysis, we performed the same numerical experiment as shown in 3.2.2, this time with all initial estimates set at 600 nm. The result shown in Fig. 22 agrees with the conclusion of our theoretical analysis. When the difference between the initial estimate and the true height is less than 90 nm, the estimated height is correct. Otherwise, it converges to a local minimum near the initial estimate. To avoid this problem, a more sophisticated optimization algorithm to find the global minimum would be required.

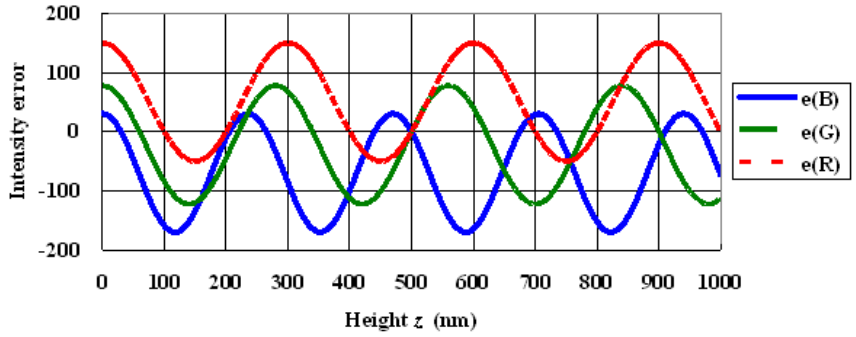

Figure 19. Intensity errors of each wavelength as a function of height, when the true height is 500 nm.

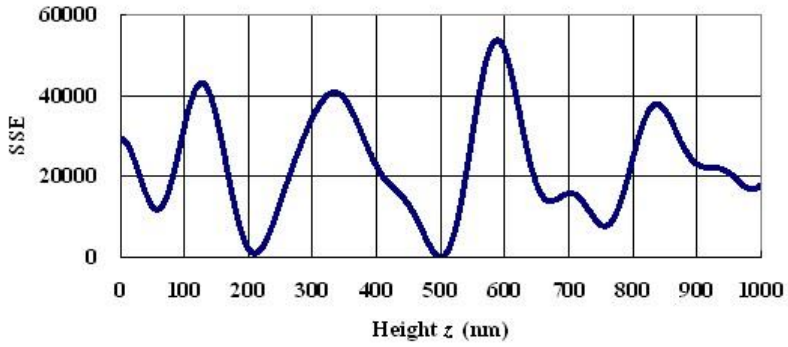

Figure 20. SSE as a function of the height, when the true height is 500 nm.

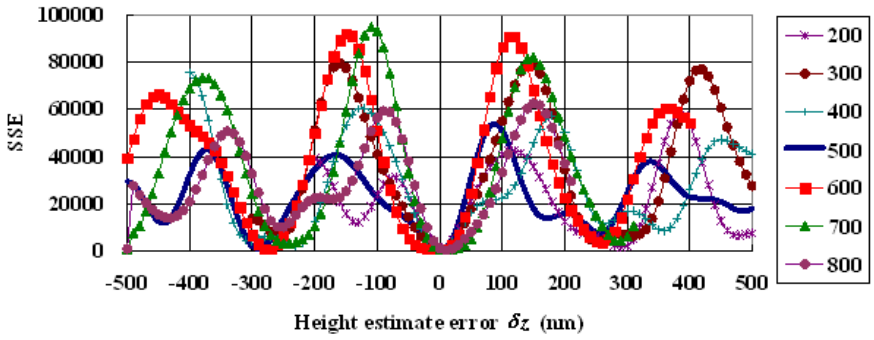

Figure 21. SSE vs. height estimate error for various true heights.

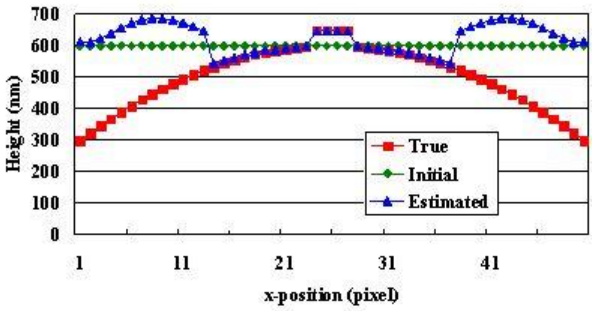

Figure 22. Estimated heights of 50 points by the GMF method

when their initial estimates are 600 nm.

6. Conclusion

We have proposed a new single-shot interferometric surface profiling technique, the Global Model Fitting (GMF) method, which enables us to measure a surface profile without the need for carrier fringes. It is based on a model-fitting algorithm and estimates the model parameters and the heights of plural points simultaneously from their multi-wavelength intensity data. When the number of the wavelengths is three, the minimum number of data points is three, and a total of nine unknown parameters including the heights of three points are estimated by least-square fitting. Once the waveform parameters are estimated by this technique, they can be used for height estimation of the points other than the fitted points, which can be executed by a much simpler and faster algorithm using the arccosine function. The validity of the proposed method has been proved by computer simulations and actual experiments.

Although this technique is applicable only to homogeneous surfaces, it has several advantages over conventional single-shot interferometry: its most significant feature is that there is no loss in spatial resolution, that is, the height of each point can be estimated independently without having to know any information about its neighboring points. Other advantages include (1) high-speed measurement, (2) low cost and simple optics without the requirement for fringe introduction, and (3) no preliminary calibration required. We are currently working on extending our technique for practical applications.

REFERENCES

[1] M. Takeda, H. Ina and S. Kobayashi, "Fourier-transform method of fringe-pattern analysis for computer-based topography and interferometry," J. Opt. Soc. Am., **72**, 156-160 (1982).

[2] S. Toyooka and M. Tominaga, "Spatial fringe scanning for optical phase measurement," Opt. Commun., **51**(2) 68-70 (1984).

[3] K.H. Womack, "Interferometric phase measurement using spatial synchronous detection," Opt. Eng., **23**, 391-395 (1984).

[4] M. Sugiyama, H. Ogawa, K. Kitagawa and K. Suzuki, "Single-shot surface profiling by local model fitting," Appl. Opt., **45**, 7999-8005 (2006).

[5] C. Quan, C.J. Tay, F. Yang and X. He, "Phase extraction from a single fringe pattern based on guidance of an extreme map," Appl. Opt., **44**, 4814-4821 (2005).

[6] K. Okada, E. Yokoyama and H. Miike, "Interference fringe pattern analysis using inverse cosine function," Electronics and Communications in Japan, Part II: Electronics, **90**(1) 61-73 (2007).

[7] K. Kitagawa, "Fast surface profiling by multi-wavelength single-shot interferometry," International Journal of Optomechatronics, **4**(2) 136-156 (2010).

[8] M. Kubo, Y. Ohtsubo, N. Kawashima and H. Marumo, "Head slider flying height measurement using a color image processing technique," Trans. of the Japan Society of Mechanical Engineers, **C 54**(503) 1401-1406 (1988).

[9] S. Hata, D. Kimura, M. Kaneda, S. Morimoto and H. Kobayashi, "Nano-level 3D shape measurement system using color analysis method of RGB interference fringes", Proc. SPIE, **8000**, 800008 (2011).

[10] C. R. Tilford, "Analytical procedure for determining lengths from fractional fringes," Appl. Opt. **16**, 1857-1860 (1977).

[11] Toray Inspection Equipment Home Page (Toray Engineering Co., 2011), http://www.scn.tv/user/torayins/

[12] R. Fletcher and M.J.D. Powell, "A rapidly convergent descent method for minimization," Computer Journal, **6**, 163-168 (1963).

Katsuichi Kitagawa received the B.E. in applied physics in 1964 from the University of Tokyo. He was an instrument and control engineer with Toray Industries, Inc. from 1964 to 2000. In 2000 he moved to Toray Engineering Co., Ltd., where he now is a Senior Adviser, Technology. He received the Ph.D. degree in Information Science and Technology from the University of Tokyo in 2011. He is a member of JSPE (the Japan Society for Precision Engineering) and SICE (the Society of Instrument and Control Engineers). He has received several awards including the SICE Technology Award in 2001, the Tejima Invention Award in 2004, and the JSPE Technology Award in 2011. He is an Advanced Measurement and Control Engineer (authorized by SICE). His current research interest is the development and application of optical interferometry.

This is the final manuscript of
Katsuichi Kitagawa, "Single-shot surface profiling by multiwavelength interferometry without carrier fringe introduction", J. Electron. Imaging 21, 021107 (May 10, 2012)

http://electronicimaging.spiedigitallibrary.org/article.aspx?articleid=1306863